DAYCENT and its land surface submodel: description and testing

William J. Parton [a,*], Melannie Hartman [a], Dennis Ojima [a], David Schimel [b]

[a] *Natural Resource Ecology Laboratory, Colorado State University, Fort Collins, CO 80523, USA*
[b] *Climate and Global Dynamics Division, National Center for Atmospheric Research, P.O. Box 3000, Boulder, CO 80303, USA*

Abstract

A land surface submodel was developed for the daily version of the CENTURY ecosystem model (DAYCENT). The goal of DAYCENT to simulate soil N_2O, NO_x, and CH_4 fluxes for terrestrial ecosystems determined the structure and processes represented in the land surface model. The land surface model was set up to simulate daily dynamics of soil water and temperature from a multi-layered soil system (0–1, 1–4, 4–15, 15–30 cm, etc.) and included surface runoff and above field capacity soil water dynamics during intense rainfall events and snowmelt into frozen soils. The comparison of the simulated soil water content (0–10 cm) with observed data from four sites was quite favorable (squared correlation coefficient—$\gamma^2 = 0.87$, 0.65, 0.86 and 0.58) and the simulated results were comparable for the soil temperature model ($r^2 = 0.92$ and 0.95 for minimum and maximum 10 cm soil temperatures). Detailed soil water and temperature data during snowmelt time periods and following rainfall events are needed to fully evaluate the performance of the water flow model. © 1998 Elsevier Science B.V. All rights reserved.

Keywords: soil water; ecological models; soil temperature; latent heat flux; DAYCENT; water flow; trace gas flux

1. Introduction

The exchange of water and energy through the land surface processes is an important component of both atmospheric and biospheric systems. The representation of these land surface exchanges of water and energy in biospheric or ecosystem models and atmospheric models, (e.g., general circulation models, GCMs) utilize various schemes of soil–vegetation processes. In atmospheric models, the land surface submodels are relatively simple in structure, yet finely resolved in time to estimate the hourly exchange of water vapor and energy to the atmosphere. Ecosystem models develop land surface submodels to control, not only the hydrological fluxes, but to determine critical controls of ecosystem processes such as plant growth, decomposition, respiration, actual evapotranspiration (AET), and trace gas fluxes. The main focus of the ecosystem land surface submodel is to estimate soil moisture dynamics and soil temperature profiles which are major environmental drivers of ecosystem processes. The level of detail represented in these ecosystem land surface submodels is often

---

* Corresponding author. Tel.: +1-970-491-1987; fax: +1-970-491-1965; e-mail: billp@nrel.colostate.edu

determined by the spatial and temporal scale of the ecosystem model. The CENTURY model (Parton et al., 1993, 1995) is a monthly time step ecosystem model and uses a modified tipping-bucket model with several soil water layers to represent the soil hydrological dynamics and various other simplified soil physical estimations to calculate soil temperature. On the other hand, in a daily time step model, such as BIOME-BGC (Running and Hunt, 1993), a more detailed land surface model is implemented to accommodate the higher temporal resolution of soil moisture and temperature changes to track the ecophysiological demands of the ecosystem representation.

A daily land surface submodel was developed for implementation in the daily version of the CENTURY model (DAYCENT). The CENTURY model has been used extensively to simulate the long-term (10–100 years) response of ecosystems to changes in climate, atmospheric CO_2 levels, and agricultural management practices (Parton et al., 1993, 1995; Parton and Rasmussen, 1994). The structure of the model and the monthly time step were appropriate to simulate the long-term ecosystem response to changes in climate, environmental factors, and land use.

The DAYCENT ecosystem model was developed to link to atmospheric models and to better estimate trace gas fluxes from different ecosystems. DAYCENT incorporates all of the ecosystem processes represented in CENTURY, however, the DAYCENT model uses the daily land surface submodel in conjunction with modified parameterization of ecosystem processes to simulate daily AET rates, plant production, nutrient cycling, and trace gas fluxes (e.g., CO_2, N_2O, NO_x, and CH_4). DAYCENT uses a more detailed set of process representation of the impacts of atmospheric CO_2 changes on ecosystem processes, the effect of atmospheric N deposition and the effect of agricultural management practices on trace gas fluxes. Mosier et al. (1996) and Parton et al. (1996a,b) showed that a daily time step was needed to represent trace gas fluxes since flux rates changed rapidly in response to changes in soil water and temperature. The current modeled and observed trace gas flux data suggest that land surface models need to use at least three soil layers in the top 15 cm of the soil and have the ability to simulate above field capacity water contents following intense rainfall events and snowmelt into frozen soils. N_2O fluxes from denitrification primarily occur during extremely wet periods, such as the snow freeze–thaw periods (Mosier et al., 1996) and are substantial part of the annual N_2O flux. Martin et al. (1998) suggest that the near surface soil water content has an impact on short term NO_x fluxes following rainfall events.

This paper will describe the land surface model used in DAYCENT and demonstrate how well the model works using observed soil temperature and water data from four sites. Soil water data (0–50 cm) and Pennman–Montieth estimated daily AET data (Goutorbe and Tarrieu, 1991; Mahfouf, 1990) from the PILPS/HAPEX site (Shao and Henderson-Sellers, 1996), soil water (0–10 cm) and measured daily AET from the CPER site (Lapitan and Parton, 1996), and soil temperature and soil water data from Germany and Scotland (Frolking et al., in press) were used to test the DAYCENT land-surface model.

2. Model description

The land surface submodel used in DAYCENT was developed by modifying existing daily water flow (Parton, 1978; Parton and Jackson, 1989; Sala et al., 1992) and soil temperature models (Parton, 1984). The soil water model was modified to simulate above field capacity water content, unsaturated water flow using Darcy's equation, runoff, snow dynamics, and the effect of soil freezing on saturated water flow. The soil temperature model was altered to include the effect of snow depth on soil surface temperature. Each soil layer (Fig. 1) was assigned unique properties including thickness, field capacity, wilting point, proportion of roots, bulk density, soil texture (percent sand and clay), saturated hydraulic conductivity, minimum water content, and pH. These values are based on observed data from each site or estimates based on soil texture at the site (Table 1). The description of the model will focus on changes to the water flow model developed by Parton (1978) and the soil temperature model developed by Parton (1984).
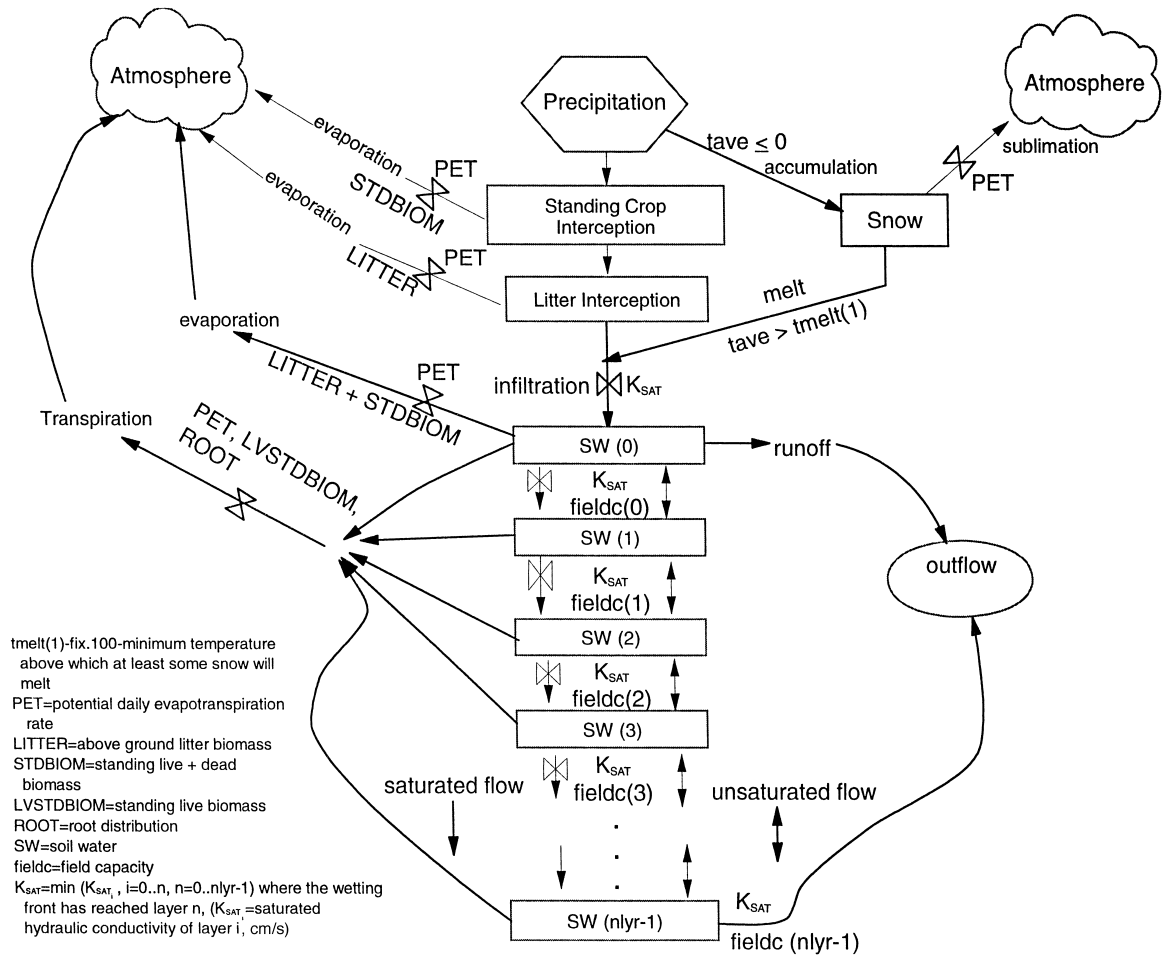
Fig. 1. Flow diagram of water flow submodel.

2.1. Water flow submodel

The water flow submodel simulates the daily flow of water through the plant canopy, litter, and soil layers. Rainfall was intercepted first by the canopy, then by the surface litter and evaporated from these surfaces (Fig. 1). Intercepted water was evaporated at the potential evapotranspiration (PET) water loss rate and the

Table 1
Site and soil characteristics (top 15 cm)

Site	Sand (%)	Clay (%)	pH	Field capacity (volume fraction)	Wilting point (volume fraction)	k_{sat} (cm/s)[a]	Depth (cm)	Crop
CPER	73	4	6.2	0.21	0.09	0.00231	150	ungrazed pasture
Scotland	37	29	6.0	0.36	0.18	0.00015	150	rye
Germany	65	10	6.2	0.31	0.12	0.00116	120	spring barley/ alfalfa/sun flower
PILPS/HAPEX	37	17	6.2	0.32	0.15	0.0014	160	soya

[a] K_{sat} = saturated hydraulic conductivity.

amount of intercepted water was a function of the plant biomass and the rainfall amount (Parton, 1978). When the air temperature was cold enough, precipitation became snow and was accumulated in a snowpack. The snowpack could be reduced by sublimation and melting. Water inputs to the soil, rainfall not intercepted and melted snow, either entered the soil or went to surface runoff. Infiltration (saturated flow), runoff, evaporation, and the redistribution of water in the soil (unsaturated flow) were based on a two-process algorithm. When there was water input, infiltration, runoff, and saturated flow were simulated first. Water was then evaporated and redistributed throughout the soil profile by an unsaturated flow algorithm modified from the work of Hillel (1977). This was followed by transpiration water loss calculated using equations developed by Parton (1978). The PET water loss rate was calculated using the equation of Penman (1948) and maximum potential transpiration and bare soil evaporation water loss were calculated as a function of live leaf biomass (bare soil evaporation decreases and transpiration increases as live leaf biomass increases; Parton, 1978). The transpiration rate was reduced under low soil water conditions as a function of the soil water potential of the wettest soil layer in the top 30 cm or the weighted average soil water potential within the plant rooting zone. Transpiration water loss from each soil layer is controlled by the soil water potential of the layer and root biomass (Parton, 1978).

On days when there was water input, a 4-h infiltration/saturated flow period was followed by ten 2-h cycles of unsaturated flow. The water input intensity (cm/s) was equal to the sum of rainfall and snowmelt (cm) divided by $4*3600$ s. When there was no water input, there were twelve 2-h cycles of unsaturated flow. The length of the infiltration/saturated flow period is a model input that can be altered, unfortunately observed data is rarely available for this driving variable.

Infiltration and saturated flow of water through the soil profile were represented by a unidirectional downward flow (Fig. 1). During infiltration the hydraulic conductivity of layer i equalled its saturated hydraulic conductivity (k_{sat_i}, cm/s) unless the layer was sufficiently cold and moist to freeze and impede water flow. A layer was considered frozen if its average soil temperature was below the freezing temperature ($-1°$C), and $\theta_{\text{sat}} - \theta_{\text{cur}} < 0.13$, where θ_{sat} was the saturated volumetric wetness of the layer and θ_{cur} was the simulated volumetric wetness (Flerchinger and Saxton, 1989). The hydraulic conductivity of a frozen layer was reduced to 0.00001 cm/s.

Initially, the rate at which water entered the soil equalled the saturated hydraulic conductivity of the top soil layer (k_{sat_0}). As water input continued the rate at which the water entered the soil and percolated downward became the minimum of the hydraulic conductivities of the soil layers that had been encountered by the wetting front. Water filled a soil layer to saturation before percolating to the next layer. If water input intensity was greater than the rate at which water could enter the soil, the difference went to runoff and was added to outflow. Water was added to the profile until the 4-h input window was over. Then if there was no impedance (frozen layer in the profile), any layer that exceeded its field capacity was drained. Starting at the top of the soil profile and progressing downward, water in excess of field capacity was drained to the layer below it. Any water that exited the bottom layer was added to outflow.

Unsaturated flow was represented by a bidirectional vertical flow (Fig. 1). At each 2-h time step, the hydraulic potential and hydraulic conductivity of each soil layer were recalculated; from these, bidirectional water fluxes and net water flux to each soil layer were computed. Based on Darcy's law, the bidirectional water flux (cm/s) between two adjacent layers, $i - 1$ and i, was calculated as:

$$\text{flux}_i = \frac{\text{dmp}_{\text{flux}} * (h_{\text{pot}i-1} - h_{\text{pot}i}) * \text{av}_{\text{cond}i}}{\text{dist}_i}, \qquad i = 1 \ldots n_{\text{lyr}} - 1 \tag{1}$$

where, dmp_{flux} is the damping multiplier, 0.000001; h_{pot_i} is the hydraulic potential of layer i (cm), the sum of the matric potential and gravitational head, where $h_{\text{pot}_i} = m_{\text{pot}_i} - \text{depth}_i$; m_{pot_i} is the matric potential of layer i (cm); depth_i is the distance from the soil surface to the middle of layer i (cm); $\text{av}_{\text{cond}_i}$ is the average hydraulic

conductivity of layer i (cm/s), a weighted average of cond_{i-1}, cond_i, and cond_{i+1}; cond_i is the hydraulic conductivity of layer i (cm/s); dist_i is the distance between the midpoints of two adjacent soil layers, $i-1$ and i (cm); n_{lyr} = the number of layers in the soil profile.

The flux at the top of the soil profile (flux_0, cm/s) was dependent on the potential soil evaporation rate ($\mathrm{pet}_{\mathrm{max}}$, cm/s), the current soilwater content of the top layer (swc_0, cm), and the minimum allowable water content in the top soil layer ($\mathrm{swc}_{\mathrm{min}_0}$, cm). The flux at the bottom of the soil profile ($\mathrm{flux}_{n_{\mathrm{lyr}}}$, cm/s) was dependent on the hydraulic conductivity of the bottom soil layer:

$$\mathrm{flux}_0 = \begin{array}{ll} -\mathrm{pet}_{\mathrm{max}}, & \mathrm{swc}_0 > \mathrm{swc}_{\mathrm{min}0} \\ 0.0, & \mathrm{swc}_0 \preceq \mathrm{swc}_{\mathrm{min}0} \end{array}$$

$$\mathrm{flux}_{n_{\mathrm{lyr}}} = \mathrm{dmp}_{\mathrm{flux}} * \mathrm{cond}_{n_{\mathrm{lyr}}-1}$$

(2)

If flux_i was positive, water moved downward from layer $i-1$ to layer i; if flux_i was negative, water moved upward from layer i to layer $i-1$. The net flux of water into or out of a layer i, n_{flux_i} (cm/s), was positive when soil layer i had a net water gain and was negative when layer i had a net water loss:

$$\mathrm{n}_{\mathrm{flux}\,i} = \mathrm{flux}_i - \mathrm{flux}_{i+1}$$

(3)

Adjustments to the bidirectional fluxes (flux_i) and net fluxes (n_{flux_i}) were computed if the addition of the net flux would have dried out a layer below its minimum allowable water content. If the addition of a net flux brought a soil layer above saturation, water in excess of saturation was added to outflow. AET from the soil was the sum of flux_0 over all time steps.

Snow accumulation, melt, and sublimation were calculated using algorithms derived from CENTURY. Precipitation accumulated in the snowpack when the average daily air temperature was below freezing. The amount of snow that melted was a product of a degree-day factor (0.125 cm/°C) and the average air temperature. Sublimation was a function of the PET rate and the latent heat of vaporization.

2.2. Soil temperature submodel

The soil temperature model, that calculates thermal diffusivity and predicts daily minimum and maximum soil temperatures at depth, was a modification of the model described in the work of Parton (1984). Required inputs to the model were daily minimum and maximum air temperatures, plant biomass, snow cover, soil moisture, soil texture, and average soil temperature at the bottom of the soil profile. In this section we have discussed the changes and augmentations to the soil temperature model described in the work of Parton (1984).

The diurnal range at the soil surface (R_s, °C) was dependent on the snow water equivalent (SWE, cm) above the soil surface and daily maximum and minimum air temperatures measured at 2 m above the soil surface ($t_\mathrm{a}^{\mathrm{mx}}$ and $t_\mathrm{a}^{\mathrm{mn}}$, °C) and was computed as:

$$R_\mathrm{s} = \begin{array}{llll} T_\mathrm{s}^{\mathrm{mx}} - T_\mathrm{s}^{\mathrm{mn}}, & \mathrm{snow} = 0, & & \\ 0.3 \quad * \quad (T_\mathrm{a}^{\mathrm{mx}} - T_\mathrm{a}^{\mathrm{mn}}), & \mathrm{snow} > 0, & \dfrac{T_\mathrm{a}^{\mathrm{mx}} + T_\mathrm{a}^{\mathrm{mn}}}{2} \succeq 0 \\ 0.3 \quad * \quad (T_\mathrm{a}^{\mathrm{mx}} - T_\mathrm{a}^{\mathrm{mn}}) \quad * \quad k_{\mathrm{snow}}, & \mathrm{snow} > 0, & \dfrac{T_a^{\mathrm{mx}} + T_a^{\mathrm{mn}}}{2} < 0 \end{array}$$

(4)

where $T_\mathrm{s}^{\mathrm{mx}}$ and $T_\mathrm{s}^{\mathrm{mn}}$ were the daily maximum and minimum soil surface temperatures (°C) described in the work of Parton (1984) and k_{snow} was the effect of snow on the diurnal range. $T_\mathrm{s}^{\mathrm{mx}}$ and $T_\mathrm{s}^{\mathrm{mn}}$ were a function of

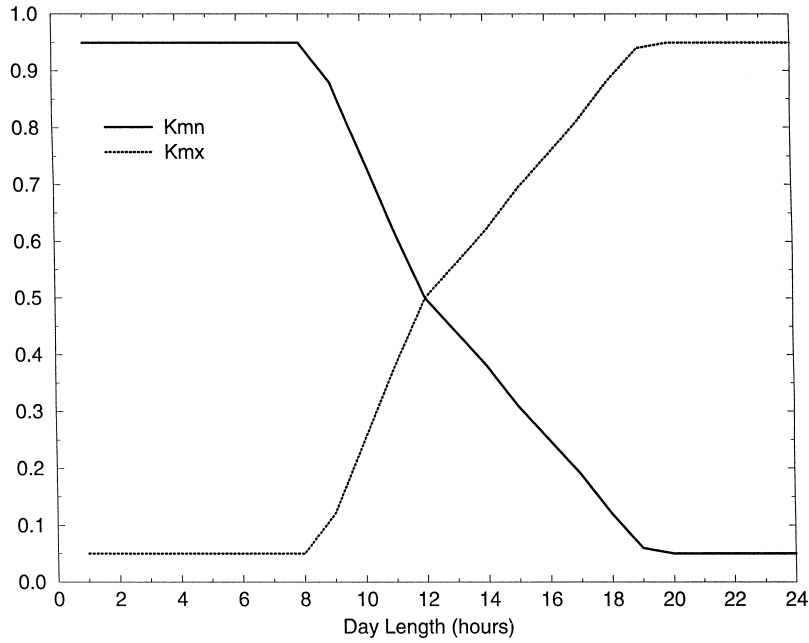## Daylength Effect on Average Soil Surface Temperature

Fig. 2. The effect of daylength on maximum surface (K_{mx}) and minimum surface (K_{mn}) temperature on average soil surface temperature.

T_a^{mx} and T_a^{mn} and plant biomass. The effect of snow, k_{snow}, on the diurnal range decreased as the SWE over the soil surface (snow, cm) increased:

$$k_{snow} = \text{maximum}((-0.15 * snow + 1.0), 0.0) \tag{5}$$

The average daily soil surface temperature (T_s^{avg}, °C) was the upper boundary for the one-dimensional Fourier heat flow equation described in the work of Parton (1984). The lower boundary temperature was site dependent and was a sine function of the annual average soil temperature at the bottom of the soil profile and Julian Date. T_s^{avg} was dependent on daylength (dl, hour), the effect of snow (k_{snow}) from Eq. (5), and air temperature (T_a^{mx} and T_a^{mn}, °C) and was calculated as:

$$T_s^{avg} = \begin{cases} K_{mx} * T_s^{mx} + K_{mn} * T_s^{mn}, & snow = 0, \\[2mm] -2, & snow > 0, \dfrac{T_a^{mx} + T_a^{mn}}{2} \geq 0 \\[2mm] -2 + 0.3 * \dfrac{T_a^{mx} + T_a^{mn}}{2} * k_{snow}, & snow > 0, \dfrac{T_a^{mx} + T_a^{mn}}{2} < 0 \end{cases} \tag{6}$$

K_{mx} and K_{mn} were the daylength effects on average soil surface temperature (Fig. 2).

3. Soil temperature and water results

The soil temperature submodel was tested by comparing simulated model results with observed data from sites in Colorado, Scotland and Germany. Comparison of the simulated and observed maximum and minimum daily 10 cm temperatures (Fig. 3a) for the Colorado Shortgrass Steppe site (CPER) show that the model
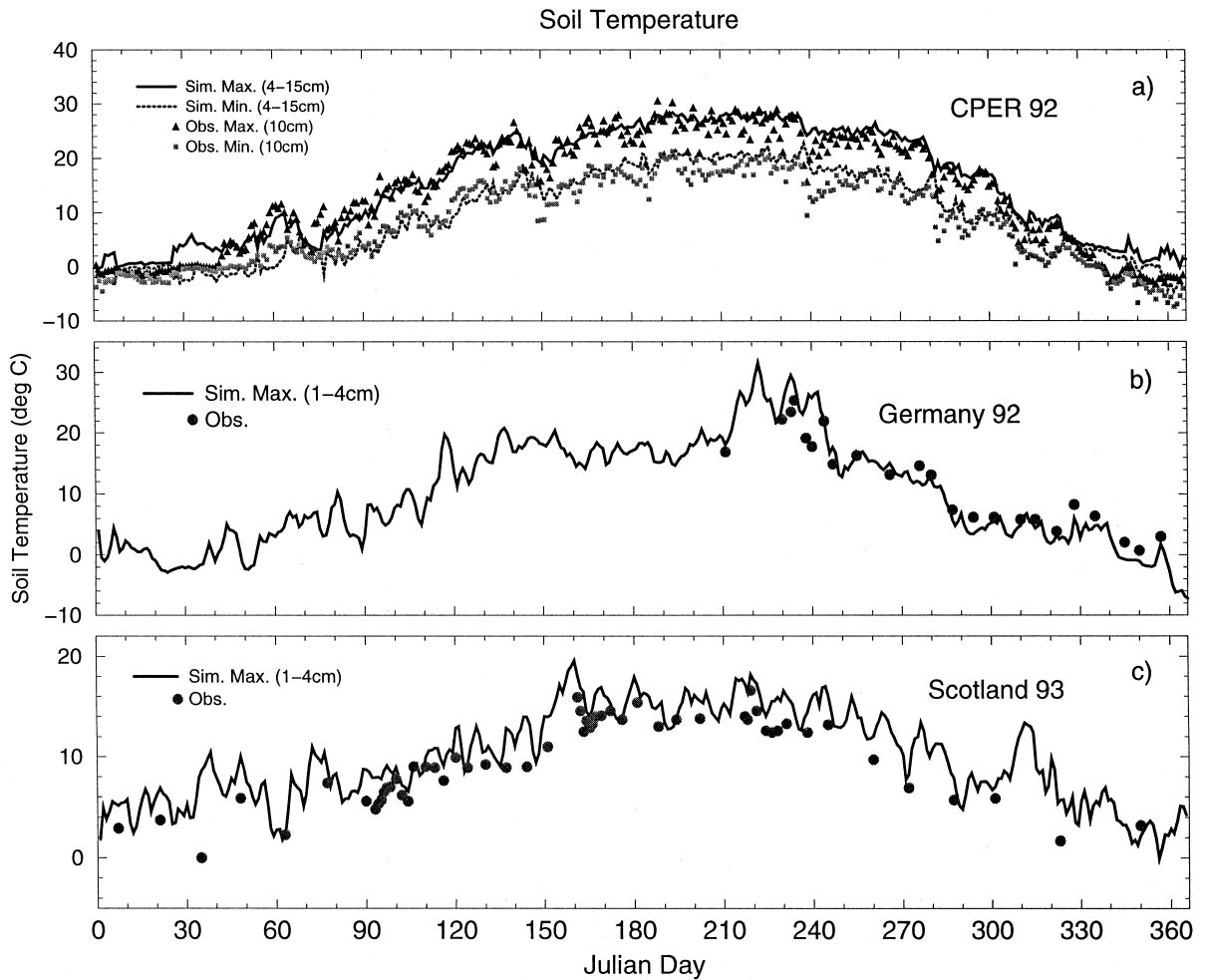
Soil Temperature

Fig. 3. (a) Comparison of observed vs. simulated 10 cm daily maximum and minimum soil temperature at CPER, (b) the comparison of observed vs. simulated soil temperature at the German site, and (c) observed vs. simulated soil temperature at the Scotland site.

simulated the daily diurnal range and seasonal patterns fairly well, with the greatest discrepancies during the winter months. Many of these errors resulted from problems in simulating snow cover and the patchy nature of observed snow cover data. Fig. 4a shows the comparison of the simulated snow amount (mm * 10) for November and December of 1992 with visually estimated daily snow cover at the CPER site. Snow cover had a big impact on both the diurnal range (snow cover decreases diurnal range) and average soil temperature (Fig. 4b and c) and thus greatly impacted predicted soil temperatures. Another factor contributing to errors were the large spatial variation in snow cover observed in the field but not represented in the model. The observed vs. simulated r^2 for the daily maximum and minimum 10 cm soil (Fig. 3a) temperature were 0.95 and 0.92, respectively.

Fig. 3b and c show the comparison of the simulated and observed soil temperature for the German and Scotland sites. The observed soil temperatures were measured weekly at different times during the day (generally during the middle of the day) and thus were compared with the simulated maximum soil temperature at 2.5 cm depth. The model did an excellent job of simulating site to site differences (lower temperatures at the

Snow Cover, Soil Temperature, and Moisture – CPER 1992
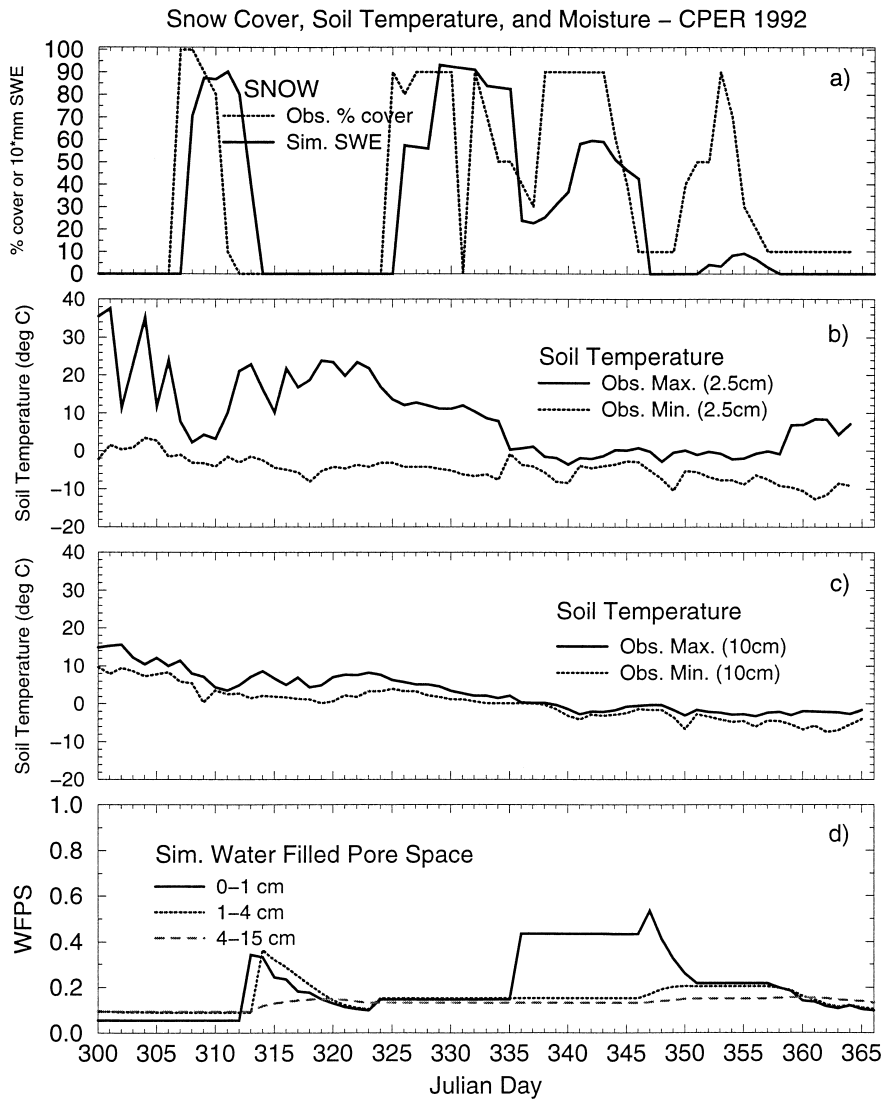

Fig. 4. Comparison of (a) visually observed snow cover with simulated SWE, (b) observed maximum and minimum 2.5 cm soil temperature, (c) observed maximum and minimum 10 cm soil temperature, and (d) simulated water filled pore space (WFPS) for the 0–1, 1–4, and 4–15 cm depths for the 1992 November and December time period at the CPER site.

Scotland site) and seasonal variations of soil temperature. The comparison with the observed data was not precise since the observed data was measured at slightly different depths and at different times during the day, however, the observed vs. simulated r^2 (0.96 and 0.88 for the German and Scotland sites) show that the model performed quite well.

The water flow submodel was tested by comparing simulated model results with observed soil water data from four sites and daily evapotranspiration data (Lapitan and Parton, 1996) from CPER and HAPEX (Goutorbe and Tarrieu, 1991). Fig. 5 shows the comparison of the simulated and observed daily AET for CPER during 1990 and 1992. The results show that the model did a good job of representing the seasonal changes in AET rates (higher during the summer compared to winter) and the short-term pattern of decreasing AET rates

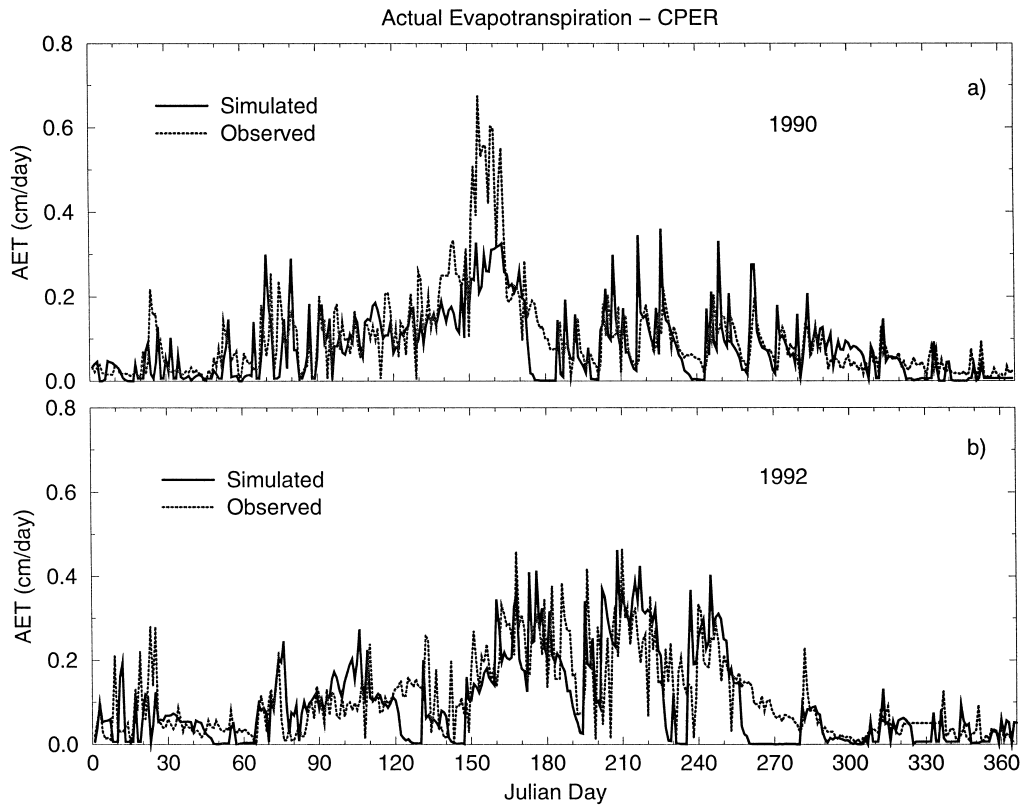Actual Evapotranspiration – CPER

Fig. 5. Simulated vs. observed AET for the CPER site during (a) 1990 and (b) 1992.

following precipitation events (see Fig. 5a from day 180 to 270). The major discrepancies in the model were the underestimate of the AET rates from day 150 to 160 (Fig. 5a) and tendency of the simulated AET rates to decrease too rapidly for certain extended dry down periods (e.g., day 250–280 in 1992) (Fig. 5b). This rapid drop off in AET rates was caused by loss of all available soil water, which could have been a result of inaccurate estimates of rainfall inputs or overestimates of AET prior to the dry down event. The underestimate of AET during June of 1990 (day 150–160) was a result of underestimating live biomass during this time period. Kelly et al. (submitted) showed that the DAYCENT model underestimated the live biomass during the 1990 May–June period (based on comparison with satellite NDVI data for the site) and thus underestimated AET rates (increasing live shoot biomass generally results in increasing AET rates). This probably resulted from the inability of the model to simulate germination of forbs and annual grasses during the 1990 spring which was quite wet. The DAYCENT model is not able to simulate year to year changes in species composition which can greatly alter biomass dynamics in certain years (Gilmanov et al., 1997). Overall, the model did a good job simulating daily AET rates with the observed vs. simulated r^2 for 1990 and 1992 equal to 0.46 and 0.42, respectively.

The simulation of soil water dynamics was tested by comparing simulated WFPS or volumetric water content (VSWC) (0–10 cm depth) with observed data. The results (Fig. 6) show that seasonal patterns of water dynamics were well simulated for all sites with the highest r^2 of observed vs. simulated data for the Scotland site ($r^2 = 0.87$), followed by the German site ($r^2 = 0.65$), and CPER site ($r^2 = 0.58$). The observed soil water data from the sites were used to estimate the field capacity and wilting point while literature estimates of water
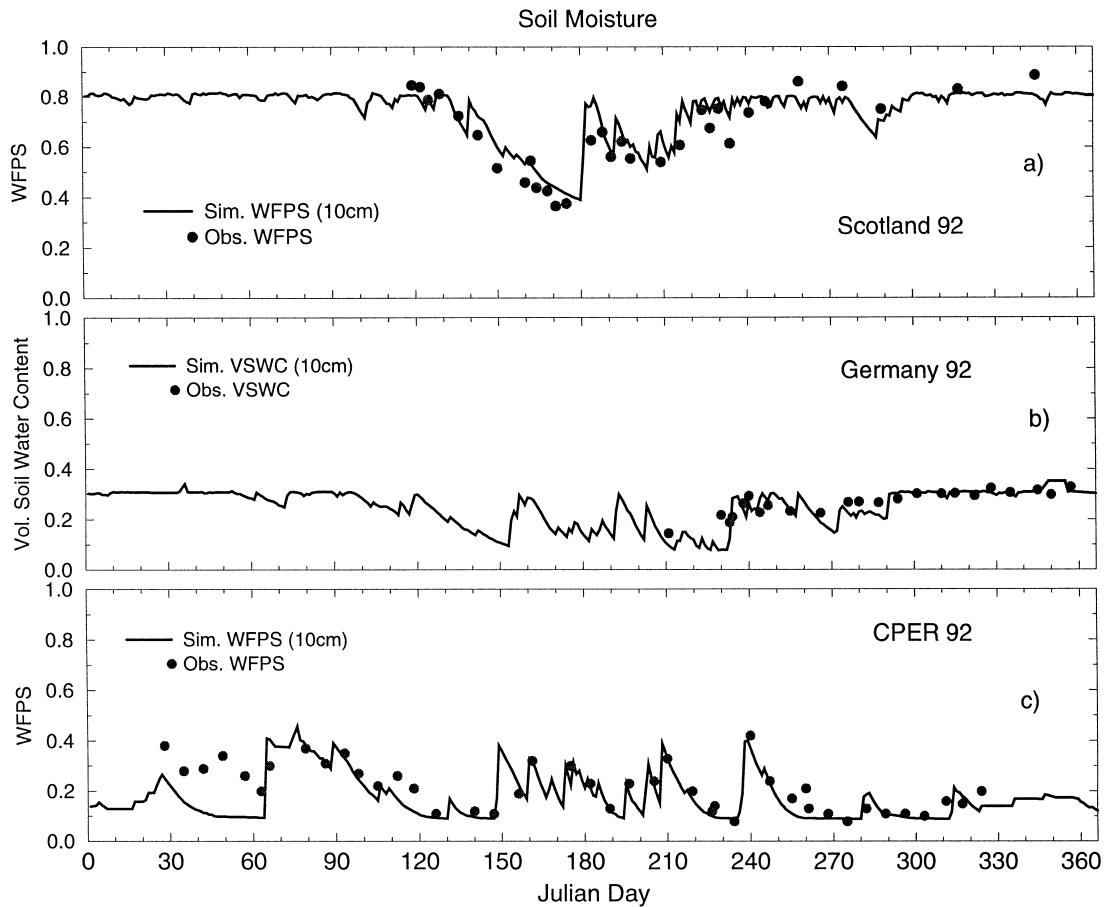
Fig. 6. Comparison of (a) observed vs. simulated WFPS (0–10 cm layer) for Scotland, (b) VSWC (0–10 cm) for Germany, and (c) WFPS (0–10 cm) for the CPER site.

potential vs. water content curves and saturated hydrologic conductivity were based on the soil texture of each site. The major discrepancy of the model was a tendency to underestimate soil water content at CPER during the winter months. It is uncertain what caused this problem, however, examination of rain gauge data from the CPER during the winter suggested that snowfall precipitation amounts were underestimated by 30 to 50%.

The comparison of simulated vs. observed soil water data (0–50 cm) for the PILPS/HAPEX site (Fig. 7a) show that the model simulates the seasonal pattern quite well with the major discrepancy being an underestimate of soil water from day 140 to 180. Fig. 7b suggests that simulated AET is overestimated from day 120 to 150 which would result in lower soil water content. The high AET rates during this time period could result from an overestimate in live leaf biomass (biomass was estimated and not measured during that time period). The comparison of simulated daily AET with estimated daily AET (Fig. 7b) shows that the model did a good job of simulating AET for the day 120 to 220 period (Fig. 7b) and AET for the whole 1986 time period ($r^2 = 0.85$, Fig. 7c). The DAYCENT land-surface model results are considerably improved for the version of the model used in the PILPS/HAPEX (Shao and Henderson-Sellers, 1996) model comparison. This is primarily a result of including unsaturated upward water flow using Darcy's equations in DAYCENT.

Fig. 4d demonstrates the ability of the water flow model to simulate above field capacity water contents during the freeze–thaw snowmelt periods. Observed trace gas data (Mosier et al., 1996) shows that denitrifica-
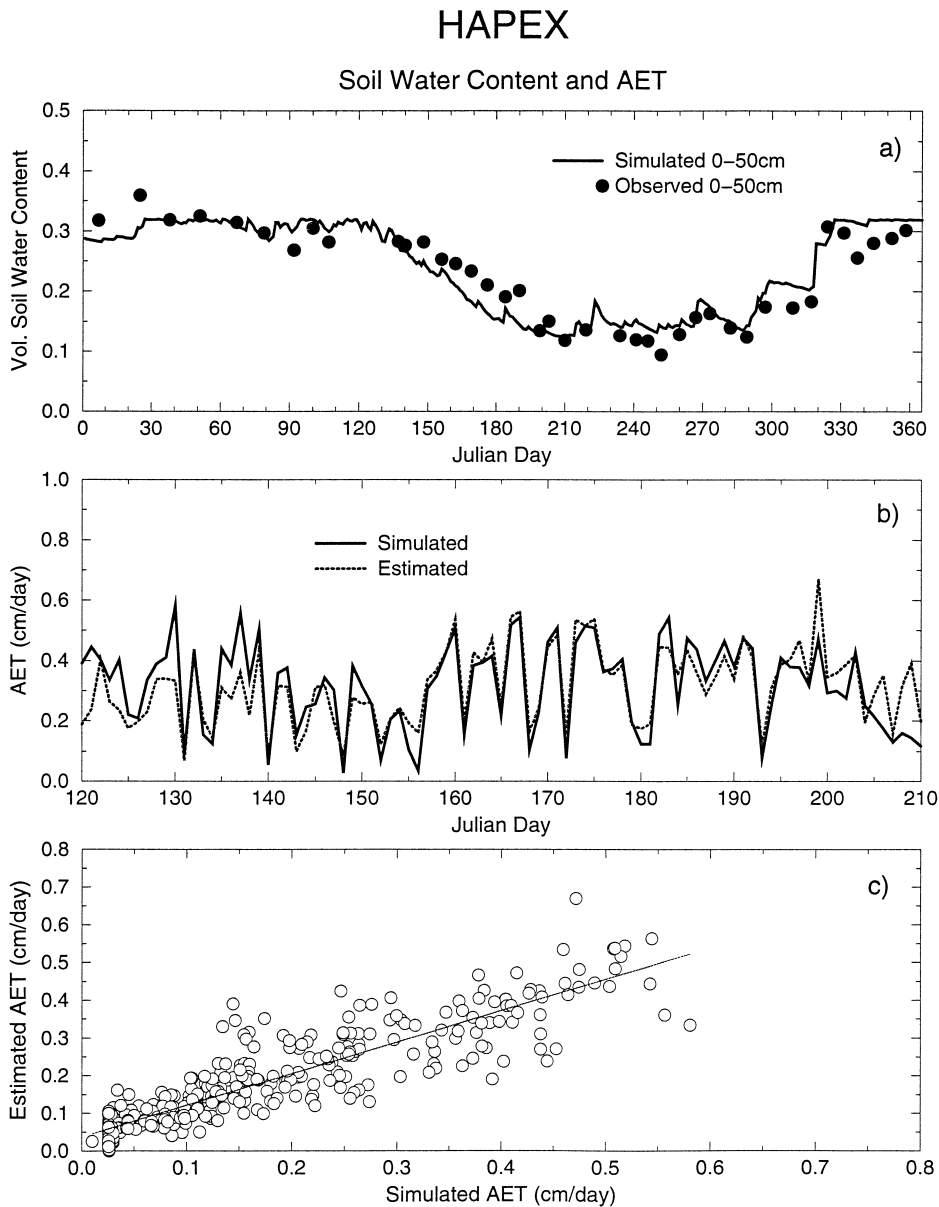
HAPEX

Soil Water Content and AET

Fig. 7. Comparison of observed vs. simulated (a) VSWC (0–50 cm depth), (b) daily AET from day 120–210, and (c) daily AET for 1986, for the PILPS/HAPEX site. The observed AET data was estimated by using a Pennman–Montieth approach (Goutorbe and Tarrieu, 1991).

tion N_2O fluxes occur during the winter months in association with freeze–thaw snowmelt periods, and contribute substantially to the annual trace gas budgets for grassland and crop systems in the Great Plains. The simulation showed that water content went above the field capacity (40% WFPS) in the 0–1 and 1–4 cm soil layers during the periods of snowmelt.

The DAYCENT model was used to simulate N_2O trace gas fluxes for the CPER, German and Scottish sites and the performance of DAYCENT trace gas model relative to other trace gas models is presented by Frolking
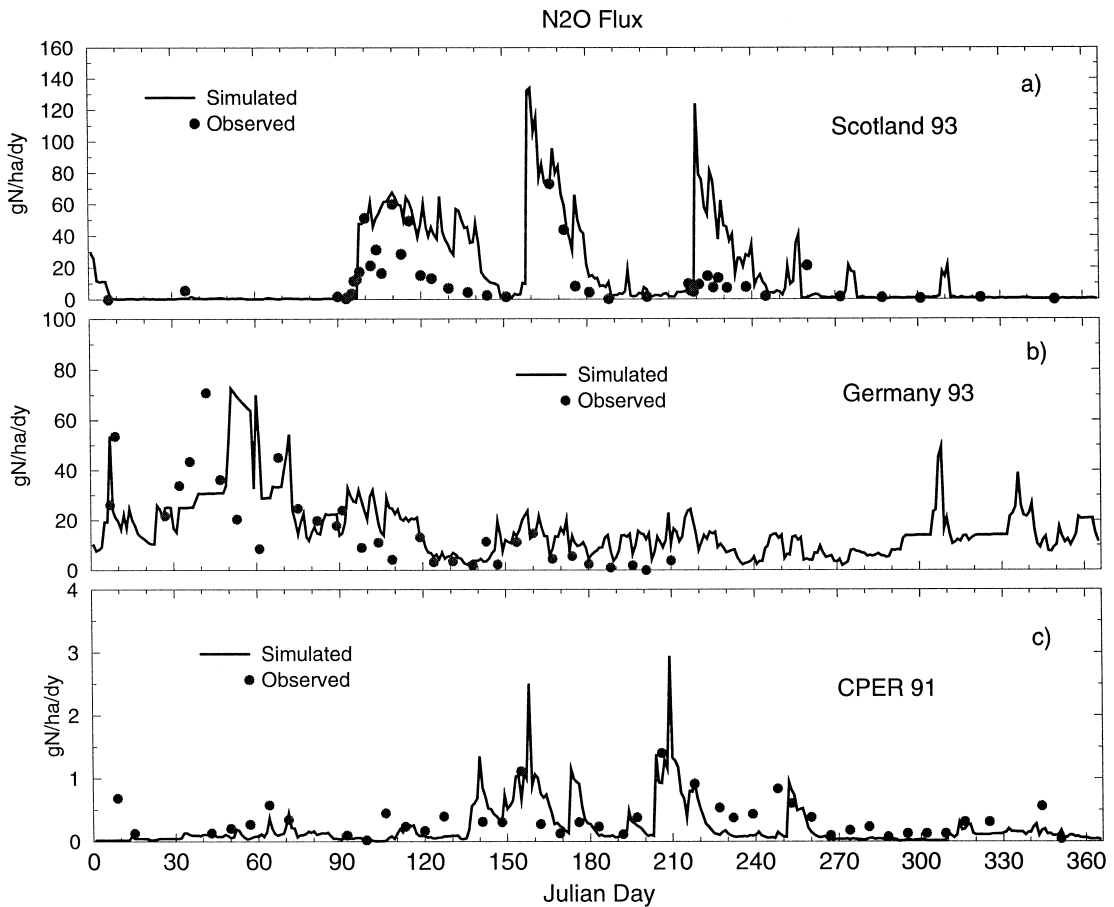
Fig. 8. Comparison of observed and simulated N_2O fluxes for the (a) Scotland, (b) Germany, and (c) CPER sites.

et al. (in press). Fig. 8 shows that the DAYCENT trace gas model correctly predicted the impact of the different management practices on N_2O fluxes. N_2O fluxes were high for the Scottish intensively fertilized grassland system and the German agricultural field that was cultivated and fertilized, while the fluxes were low from the natural grassland site in Colorado. Frolking et al. (in press) demonstrated that the DAYCENT model correctly simulated the mean annual N_2O flux for different treatments at the three sites, however, there were time periods when the model results were quite different from the observed data and time periods when the model results compared quite well with the observed data. The reason for the discrepancies is not clear, and the different models perform well during different time periods. It is important to note that ecosystem models need to simulate plant growth, nutrient uptake, nutrient mineralization, and soil water and temperature dynamics well in order to simulate trace gas fluxes and that an error in any one of these simulated processes can lead to errors in the trace gas predictions.

4. Discussion

This paper demonstrates that the DAYCENT land surface submodel did a good job of simulating soil water and soil temperature dynamics for a variety of sites ranging from a dry grassland, wet managed grassland, and

wet crop land systems. The simulated results were compared with observed snow cover data, weekly 0–10 cm soil water data, daily AET data, and soil temperature data. The model simulated the observed changes in soil water content following precipitation events for different times of year with the observed vs. simulated r^2 of 0.58, 0.65, 0.87 and 0.86, respectively, for the CPER, German, Scotland and PILPS/HAPEX sites. The r^2 for the observed vs. simulated daily AET rates at the CPER sites were 0.46 (1990) and 0.42 (1992) and at the PILPS/HAPEX site 0.85. The r^2 for soil temperature observed vs. simulated comparisons for the maximum and minimum 10 cm soil temperature at CPER were 0.95 and 0.92, respectively, and the r^2 was 0.96 and 0.88 for the soil temperatures observed at the German and Scotland sites. For calibration purposes, the observed soil water data was only used to estimate the field capacity and wilting point (Table 1). Maximum and minimum soil temperature for 1 year at the CPER site were used to estimate the effect of day length on average daily soil surface soil temperatures (Fig. 2).

The major discrepancy between the observed and simulated soil temperature data was a tendency to overestimate 10 cm soil temperature at the CPER site during the winter months. It is unclear what caused the problem but spatial and temporal variability in snow cover contributed to the discrepancy. The soil water model also tended to underestimate the 0–10 cm soil water content during the winter months at the CPER site. This error was likely a result of underestimating water inputs by 30–50% during snow storms. The water flow submodel also underestimated daily AET rates during early June of 1990, which was probably a result of an underestimate of live plant biomass by the plant production model. In general, the model results compared quite favorably with the observed data, however, it is difficult to evaluate how well models perform without a model comparison activity like the effort used in PILPS model comparisons (Shao and Henderson-Sellers, 1996).

Data from nutrient cycling, trace gas flux and decomposition studies (Mosier et al., 1996; Parton et al., 1996a,b; Schimel and Parton, 1986; etc.) show that the structure and time steps required for land surface models depend on the biogeochemistry process represented in the model. For example, Parton et al. (1996a,b) showed that a detailed, near surface soil layer structure is needed to represent decomposition and nutrient cycling since most of the nutrient cycling and soil respiration occur in the top 15 cm of the soil. Mosier et al. (1996) and Parton et al. (1996a,b) have shown that denitrification N_2O losses are a substantial part of total annual N_2O losses and occur when soil water content is near or above field capacity. These conditions primarily occurred during the freeze–thaw period associated with snowmelt. The DAYCENT land surface submodel has been set up to simulate these conditions. The NO_x trace gas flux data (Martin et al., 1998) suggested that the rapid drying of the soil water content in the 0–4 cm layer was associated with the observed rapid decrease in NO_x following the precipitation event. The observed NO_x and denitrification data suggest that detailed soil water and temperature data at 0–5 cm, 5–10 and 10–15 cm layers are needed following rainfall events during the summer and freeze–thaw snowmelt periods in order to accurately test a land surface model. This type of data is difficult to find. With the snowmelt process, there are further problems since snow distributions in the field are rarely uniform, and the model generally represents the average snow amount and does not deal with the spatial variation in snow cover.

This paper demonstrates that input data requirements, validation data, structure of the land surface model and resolution of the models are greatly impacted by the ecosystem processes represented in linked land surface-ecological models and that more detailed process-oriented land surface models are required if trace gas fluxes are considered.

Acknowledgements

References

Flerchinger, G.N., Saxton, K.E., 1989. Simultaneous heat and water model of freezing snow-residue–soil system: I. Theory and development. Trans. ASAE 32, 565–571.

Frolking, S., Moser, A.R., Ojima, D.S., Li, C., Potter, C.S., Parton, W.J., Priesack, E., Smith, K.A., Flessa, H., Stenger, R., Haberbosch, C., Doersch, P., in press. Comparison of N_2O emissions from soils at three temperate agricultural sites: year-round measurements and simulations by four models. Nutr. Cycling Agroecosys.

Gilmanov, T.G., Parton, W.J., Ojima, D.S., 1997. Testing the 'CENTURY' ecosystem model on data sets from eight grassland sites in the former USSR representing a wide climatic/soil gradient. Ecolog. Model. 96, 191–210.

Goutorbe, J.P., Tarrieu, C., 1991. HAPEX-MOBILHY data base. In: Schmugge, Andre (Eds.), Land Surface Evaporation. Springer-Verlag, Berlin, pp. 415–426.

Hillel, D., 1977. Computer Simulation of Soil–Water Dynamics: A Compendium of Recent Work. International Development Research Center, Ottawa, Canada, pp. 90–94.

Kelly, R.H., Parton, W.J., Hartman, M.D., Stretch, L.K., Ojima, D.S., Schimel, D.S., submitted. Intra- and interannual variability of ecosystem processes in shortgrass steppe: new model, verification, simulations. Global Change Biol.

Lapitan, R.L., Parton, W.J., 1996. Seasonal variabilities in the distribution of the microclimatic factors and evapotranspiration in a shortgrass steppe. Agric. For. Meteorol. 79, 113–130.

Mahfouf, J.F., 1990. A numerical simulation of the surface water budget during HAPEX-MOBILHY. Boundary Layer Meteorol. 53, 201–222.

Martin, R.E., Scholes, M.C., Mosier, A.R., Ojima, D.S., Holland, E.A., Parton, W.J., 1998. Controls on annual emissions of nitric oxide from soils of the Colorado shortgrass steppe. Global Biogeochem. Cycles 12, 81–91.

Mosier, A.R., Parton, W.J., Valentine, D.W., Ojima, D.S., Schimel, D.S., Delgado, J.A., 1996. CH_4 and N_2O fluxes in the Colorado shortgrass steppe: I. Impact of landscape and nitrogen addition. Global Biogeochem. Cycles 10, 387–399.

Parton, W.J., 1978. Abiotic section of ELM. In: Innis, G.S. (Ed.), Grassland Simulation Model. Ecological Studies Analysis and Synthesis, 45, pp. 31–53.

Parton, W.J., 1984. Predicting soil temperatures in a shortgrass steppe. Soil Sci. 138, 93–101.

Parton, W.J., Jackson, L., 1989. Simulated water budgets for an annual grassland site in the Sierra Foothills. In: Huenneke, L.F., Mooney, H. (Eds.), Grassland Structure and Function: California Annual Grassland. Kluwer Academic Publishers, Dordrecht, The Netherlands, pp. 163–171.

Parton, W.J., Rasmussen, P.E., 1994. Long-term effects of crop management in wheat–fallow: II. CENTURY model simulations. Soil Sci. Soc. Am. J. 58, 530–536.

Parton, W.J., Scurlock, J.M.O., Ojima, D.S., Gilmanov, T.G., Scholes, R.J., Schimel, D.S., Kirchner, T., Menaut, J.-C., Seastedt, T., Garcia Moya, E., Kamnalrut, A., Kinyamario, J.I., 1993. Observations and modeling of biomass and soil organic matter dynamics for the grassland biome worldwide. Global Biogeochem. Cycles 7, 785–809.

SCOPEGRAM Group Members, Parton, W.J., Scurlock, J.M.O., Ojima, D.S., Schimel, D.S., Hall, D.O., 1995. Impact of climate change on grassland production and soil carbon worldwide. Global Change Biol. 1, 13–22.

Parton, W.J., Haxeltine, A., Thornton, P., Anne, R., Hartman, M., 1996a. Ecosystem sensitivity to land-surface models and leaf area index. Global Planet. Change 13, 89–98.

Parton, W.J., Mosier, A.R., Ojima, D.S., Valentine, D.W., Schimel, D.S., Weier, K., Kulmala, A.E., 1996b. Generalized model for N_2 and N_2O production from nitrification and denitrification. Global Biogeochem. Cycles 10, 401–412.

Penman, H.L., 1948. Natural evaporation from open water, bare soil and grass. Proc. R. Soc. London, Ser. A. 193, 120–145.

Running, S.W., Hunt, E.R., Jr., 1993. Generalization of a forest ecosystem process model for other biomes, BIOME-BGC, and an application for global-scale models. In: Ehleringer, J.R., Field, C. (Eds.), Scaling Processes Between Leaf and Landscape Levels. Academic Press, Orlando, pp. 141–158.

Sala, O.E., Lauenroth, W.K., Parton, W.J., 1992. Long-term soil water dynamics in the shortgrass steppe. Ecology 73, 1175–1181.

Schimel, D.S., Parton, W.J., 1986. Microclimate controls of N mineralization and nitrification in shortgrass steppe soils. Plant Soil 93, 347–357.

Shao, Y., Henderson-Sellers, A., 1996. Validation of soil moisture simulation in landsurface parameterization schemes with HAPEX data. Global Planet. Change 13, 11–46.